

RESEARCH

Open Access



# Knockdown of ribosome RNA processing protein 15 suppresses migration of hepatocellular carcinoma through inhibiting PATZ1-associated LAMC2/FAK pathway

Tongtong Pan<sup>2†</sup>, Jinhai Li<sup>3†</sup>, Ouyang Zhang<sup>1</sup>, Yuqin Zhu<sup>1</sup>, Hongfei Zhou<sup>2</sup>, Mengchen Ma<sup>1</sup>, Yanwen Yu<sup>1</sup>, Jiaojian Lyu<sup>4</sup>, Yongping Chen<sup>2\*</sup> and Liang Xu<sup>1\*</sup>

## Abstract

**Background** Ribosomal RNA processing protein 15 (RRP15) has been found to regulate the progression of hepatocellular carcinoma (HCC). Nevertheless, the extent to which it contributes to the spread of HCC cells remains uncertain. Thus, the objective of this research was to assess the biological function of RRP15 in the migration of HCC.

**Methods** The expression of RRP15 in HCC tissue microarray (TMA), tumor tissues and cell lines were determined. In vitro, the effects of RRP15 knockdown on the migration, invasion and adhesion ability of HCC cells were assessed by wound healing assay, transwell and adhesion assay, respectively. The effect of RRP15 knockdown on HCC migration was also evaluated in vivo in a mouse model.

**Results** Bioinformatics analysis showed that high expression of RRP15 was significantly associated with low survival rate of HCC. The expression level of RRP15 was strikingly upregulated in HCC tissues and cell lines compared with the corresponding controls, and TMA data also indicated that RRP15 was a pivotal prognostic factor for HCC. RRP15 knockdown in HCC cells reduced epithelial-to-mesenchymal transition (EMT) and inhibited migration in vitro and in vivo, independent of P53 expression. Mechanistically, blockade of RRP15 reduced the protein level of the transcription factor POZ/BTB and AT hook containing zinc finger 1 (PATZ1), resulting in decreased expression of the downstream genes encoding laminin 5 subunits, LAMC2 and LAMB3, eventually suppressing the integrin  $\beta$ 4 (ITGB4)/focal adhesion kinase (FAK)/nuclear factor  $\kappa$ B kappa-light-chain-enhancer of activated B cells (NF- $\kappa$ B) signaling pathway.

<sup>†</sup>Tongtong Pan, Jinhai Li authors contributed equally to this work.

\*Correspondence:  
Yongping Chen  
cyp@wmu.edu.cn  
Liang Xu  
liangxu1023@gmail.com

Full list of author information is available at the end of the article



© The Author(s) 2024. **Open Access** This article is licensed under a Creative Commons Attribution 4.0 International License, which permits use, sharing, adaptation, distribution and reproduction in any medium or format, as long as you give appropriate credit to the original author(s) and the source, provide a link to the Creative Commons licence, and indicate if changes were made. The images or other third party material in this article are included in the article's Creative Commons licence, unless indicated otherwise in a credit line to the material. If material is not included in the article's Creative Commons licence and your intended use is not permitted by statutory regulation or exceeds the permitted use, you will need to obtain permission directly from the copyright holder. To view a copy of this licence, visit <http://creativecommons.org/licenses/by/4.0/>. The Creative Commons Public Domain Dedication waiver (<http://creativecommons.org/publicdomain/zero/1.0/>) applies to the data made available in this article, unless otherwise stated in a credit line to the data.

**Conclusions** RRP15 promotes HCC migration by activating the LAMC2/ITGB4/FAK pathway, providing a new target for future HCC treatment.

**Keywords** Ribosome RNA processing protein 15, Hepatocellular carcinoma migration, LAMC2, Focal adhesion kinase

## Introduction

Globally, liver cancer is the 6th most common malignancy and the 3rd leading cause of cancer-related fatalities. Hepatocellular carcinoma (HCC) stands as the prevailing form of liver cancer, with around 900,000 new cases and 820,000 fatalities recorded in 2020 alone [1]. Despite significant advances in therapeutic strategies such as surgical resection, radiofrequency ablation, liver transplantation and immunotherapy, the overall prognosis of HCC is still poor [2, 3], with the majority of patients suffering from postoperative recurrence, invasion and metastasis [4]. Extrahepatic metastases have been reported to occur in 13.5–42% of HCC cases [5], and the most common sites of blood metastasis are the lungs (up to 60% of patients with metastatic disease) and bone (up to 40% of patients) [5–7]. Hence, clarifying the specific mechanisms of cellular metastasis in HCC and finding new targets are critical to improving the survival of HCC patients.

Tumor cell interaction with the extracellular matrix (ECM) is a well-recognized link leading to tumor progression [8], which forms the scaffolding for tissues and provides structural integrity. The ECM promotes tumor metastasis through the formation of focal adhesions with the integrins on the tumor cell membrane [9, 10] via glycoproteins such as the laminins [11]. Laminin-5, encoded by the LAMA3, LAMB3 and LAMC2 genes, is the primary adhesion component of the epidermal basement membrane. Laminin 5 interacts with integrins  $\alpha3\beta1$  or  $\alpha6\beta4$  on tumor cells to activate focal adhesion kinase (FAK) and nuclear factor kappa-light-chain-enhancer of activated B cells (NF- $\kappa$ B), which promotes tumor cell migration and invasion [12–14].

Ribosome RNA processing protein 15 (RRP15) is a nucleolar protein required for nucleole formation [15]. A recent study showed that ribosome biogenesis is accompanied by an increase in RRP15 levels, suggesting that the latter could be a significant factor in carcinogenesis [16]. Knocking down RRP15 in cancer cells resulted in cell cycle arrest or apoptosis [15]. Deficiency of RRP15 decreased the proliferation and metastasis of colorectal cancer cells [17, 18]. Although inhibition of RRP15 has been found to inhibit HCC proliferation and growth [19], the function of RRP15 in HCC metastasis has not yet been revealed [20]. Hence, this research sought to elucidate the function of RRP15 in the migration of HCC cells, and explore the underlying mechanisms.

## Materials and methods

### Data

RNA-seq expression matrices from HCC and normal samples was obtained from GEPIA database (<http://gepia.cancer-pku.cn/>).

### Patients

Tumors and matched peritumoral specimens were donated by 20 patients with HCC who underwent surgical resection without preoperative treatment at Lishui People's Hospital (Lishui, Zhejiang, China), who were informed of the objective of the study and gave informed consent. This research was granted approval by the Ethics Committee of the Lishui People's Hospital (No. LLW-FO-401). 20 pairs of liver tissues were homogenized for total RNA extraction, and 12 pairs were used for protein isolation.

### Tissue microarrays and immunohistochemistry assay

The tissue microarray (TMA) was purchased from YEP-COME Biotechnology (YP-LVCSUR1801, Shanghai, China), consists of a total of 79 formalin-fixed and paraffin-embedded tissue sections. The TMA sections were stained with rabbit anti-RRP15 sera were applied at 1:50 dilution [17], and the expression level of RRP15 was scored according to the signal intensity and distribution. The specific methods and scoring rules were described previously [21].

### Cell lines and cell culture

The HepG2 cells were purchased from ATCC (Washington D.C., USA), and the Huh7, MHCC-97 H, MHCC-97 L and LM3 cell lines were purchased from the Chinese Academy of Sciences' Cell Bank (Shanghai, China). MIHA cell line was purchased from the Hunan Fenghui Biotechnology Co., Ltd (CL0469, Hunan, China). Cell lines were cultivated according to the instructions and passaged at 80% fusion.

### Small interfering RNA (siRNA) and short hairpin RNA (shRNA) transfection

SiRNAs targeting RRP15, LAMC2 and PATZ1, and the RRP15 shRNA were bought from GenePharma Company (Shanghai, China). The sequences are listed in Supplementary Table 1. ShRNA and negative control were separately cloned into pLKO.1-puro vectors (Sigma-Aldrich, Burlington, MA, USA). Full length RRP15 (NM\_016052.4) cDNA was synthesized and cloned into the expression vector pCDH (Sigma-Aldrich). Cells were

transfected with the respective constructs (50nM siRNAs) using Lipofectamine 3000 reagent (Invitrogen, Carlsbad, CA, USA).

#### Wound healing assay

The transfected cells were cultured in six-well plates, and the monolayers were scraped longitudinally with a sterile 10- $\mu$ L pipette tip once the cells were 80–90% confluent. After rinsing the cell debris with PBS, the adherent cells were cultivated in serum-free medium, and photographs of the wound area were taken at 12 h intervals over a period of 48 h to assess cell migration.

#### Transwell migration and invasion assay

$8 \times 10^4$  cells were inoculated into the upper chamber of each well of a transwell plate (24 wells, 8  $\mu$ m pore size; Corning, New York, USA) with 200  $\mu$ L of serum-free medium and the lower chamber with medium containing 10% FBS. For the invasion assay, the cells were seeded in transwell filters pre-coated with 30  $\mu$ L diluted (1:9) Matrigel (Corning). After incubating for 36 h, the cells remaining on the surface of the filter were removed, and those that had migrated/invaded were fixed with 4% paraformaldehyde (PFA) and stained with crystal violet (Beyotime Biotechnology, Shanghai, China). The count of migrated or invaded cells was counted in 5 random fields per well.

#### Cell adhesion assay

MHCC-97 H and LM3 cells were seeded into 96-well plates pre-coated with Matrigel at the density of  $8 \times 10^3$  cells/well. After 1 h, the plates were rinsed with PBS, the attached cells were fixed with 4% PFA and stained with Wright's Giemsa (Beyotime Biotechnology). The cells were photographed and counted under a microscope.

#### Cell proliferation assay

MHCC-97 H and LM3 cells were inoculated into 96-well plates at a density of  $2 \times 10^3$  cells/well, and then transfected with different siRNAs (siNT/siRRP15-1/siRRP15-2) or treated with 5  $\mu$ M Sorafenib (Solarbio Life Sciences, Beijing, China), and cultured for 24, 48, 72, 96 and 120 h respectively. 10  $\mu$ L of Cell Counting Assay Kit 8 Reagent (CCK-8; Dojindo Laboratories, Kumamoto, Japan) was added to each well for incubation. Spectrophotometers (Varioskan Flash, Thermo Fisher Scientific, Waltham, MA, USA) were used to measure absorbance at 450 nm and to calculate the percentage of living cells.

#### Colony formation assay

The cells were inoculated into a 6-pore panel at a 1000 cells/well. After 14 days, the colonies were washed twice with PBS, fixed with 4% PFA, stained with crystal violet (Beyotime Biotechnology), and counted.

#### Apoptosis assay

MHCC-97 H and LM3 cells were inoculated in 24-well plates at a density of  $2 \times 10^4$  cells/well and transfected with different siRNAs (siNT/siRRP15-1/siRRP15-2). Apoptosis was assessed by flow cytometry (Becton Dickinson FACS Calibur; BD Biosciences, Franklin Lakes, NJ, USA) analysis according to the instructions of Annexin V-PE / 7-AAD Apoptosis Detection Kit (KeyGEN Biotech, Nanjing, China).

#### Cell cycle assay

MHCC-97 H and LM3 cells were seeded in 24-well plates at the density of  $2 \times 10^4$  cells/well, and transfected with different siRNAs (siNT/siRRP15-1/siRRP15-2). After culturing for 48 h, the cells were collected into single cells, rinsed with ice-cold PBS and fixed overnight with chilled 70% ethanol at  $-20^\circ\text{C}$ . The cells were washed twice with PBS and incubated with 50  $\mu$ g/mL propidium iodide (Solarbio Life Sciences, Beijing, China) and 0.1 mg/mL RNase A (Qiagen, Hilden, Germany) in PBS. The stained cells were analyzed in a flow cytometer.

#### Establishment of in vivo tumor models

Male BALB/c nude mice (age: 5–6 weeks; weight: 18–22 g; SLAC Laboratory Animal Co. Ltd., Shanghai, China) were randomly divided into the RRP15 knock-down and control groups. The mice were injected with  $3 \times 10^6$  MHCC-97 H cells in 100  $\mu$ L PBS and 100  $\mu$ L Matrigel to create subcutaneous tumors in their right axillary fossa. The tumors were measured every 3 days using calipers, and tumor volume was calculated as  $(\text{length} \times \text{width}^2)/2$ . The migration model involved the injection of  $1 \times 10^7$  MHCC-97 H cells in 100  $\mu$ L PBS into the mice's tail vein. Eight weeks after inoculation, mice were euthanized by  $\text{CO}_2$  asphyxiation, and the lungs were dissected [22]. The tissues were fixed with 4% PFA, embedded in paraffin, and stained with hematoxylin and eosin (H&E). Animal experiments were approved by the Wenzhou Medical University Animal Experiment Committee (No. wyd2022-0164).

#### RNA-sequencing analysis

TRIzol™ reagent (Invitrogen) was utilized to extract total RNA from MHCC-97 H cells. LC-Bio Technology CO. Ltd. (Hangzhou, China) conducted RNA-sequencing. The entirety of the sequencing data produced in this research has been stored in the GEO database (GSE228416).

#### mRNA and protein detection

Total RNA and protein were extracted from cells using TRIzol™ reagent (Invitrogen) and RIPA lysis buffer (Millipore, Billerica, Massachusetts, USA), respectively. Real-time PCR analyses were performed according to manufacturers' instructions. Primers used for real-time

PCR were shown in Supplementary Table S2. The expression of proteins was determined with immunoblotting. Briefly, proteins were separated by sodium dodecyl sulfate-polyacrylamide gel electrophoresis, transferred onto polyvinylidene fluoride or polyvinylidene difluoride membranes (Millipore). Then, the membrane was cut into strips and incubated overnight with primary antibodies at 4 °C (Supplementary Table 3). Blots were detected by chemiluminescence (Bio-Rad, Hercules, CA, USA) and visualized using Image Lab software (version 6.1, Bio-Rad Laboratories).

### Statistical analyses

Data were analyzed using GraphPad Prism 8 software (San Diego, CA). The experimental data were presented as the mean  $\pm$  standard error of the mean (SEM) of three independent experiments performed in triplicate. Student's *t* test and one-way analysis of variance (ANOVA) were used to compare data between groups, and *p*-value < 0.05 was considered statistically significant.

## Results

### RRP15 was upregulated in HCC tissues and cells

RRP15 mRNA was significantly upregulated in HCC samples compared to normal liver samples in the GEPIA database (Fig. 1A). In addition, analysis of the Kaplan-Meier database revealed that high RRP15 expression was significantly associated with lower overall survival (Fig. 1B). We also evaluated RRP15 mRNA and protein levels in paired HCC and normal liver tissue samples, revealing a significant elevation in RRP15 expression within HCC tissues (Fig. 1C, D). RRP15 expression profile was accessed by IHC in a human TMA containing 79 paired HCC and peritumor tissues and representative images were shown in Fig. 1E. The results indicated that RRP15 were scored as positive expression in 36.53% of HCC tissues, as compared with 24.83% of corresponding peritumor tissues (Fig. 1E). It was further found that there was no significant difference in the protein levels of RRP15 between non-HBV-HCC patients and HBV-HCC patients (Supplementary Fig. 1A). We subsequently examined its mRNA and protein levels in five HCC cell lines (HepG2, Huh7, MHCC-97 L, MHCC97-H and LM3) as well as MIHA cells. As expected, all HCC cell lines were enriched in RRP15 compared to the control (Fig. 1F, G). In addition, we determined RRP15 expression from TCGA data based on the four major HCC etiologies, including HBV, HCV, alcoholic steatohepatitis, and non-alcoholic steatohepatitis. The results showed that the expression of RRP15 was comparable among the four HCC etiologies (Supplementary Fig. 1B). These findings suggest that RRP15 may be closely associated with HCC deterioration. In order to ascertain the involvement of RRP15 in HCC migration, we opted to conduct

subsequent experiments on the metastatic MHCC-97 H and LM3 cell lines.

### RRP15 knockdown inhibited the proliferation and induced apoptosis of HCC cells

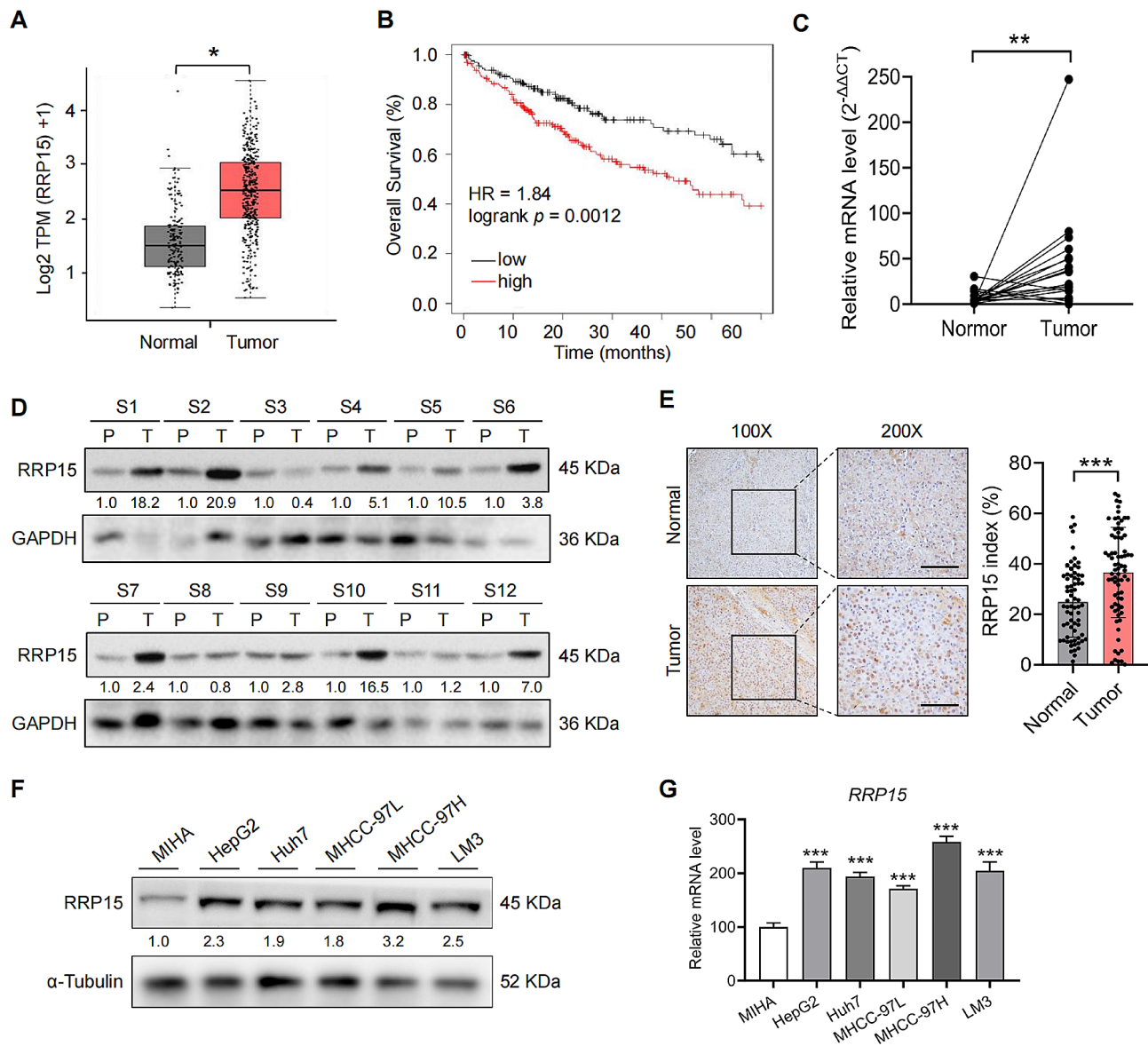
We induced gene knockdown in the MHCC-97 H and LM3 cell lines using specific siRNAs to assess the involvement of RRP15 in HCC cell progression (Supplementary Fig. 2A–B). RRP15 depletion led to a substantial decline in viability compared with that in the respective controls after 48 h of culture (Supplementary Fig. 2C). Furthermore, RRP15 knockdown resulted in a decrease of 70.4% and 36.4% in the colonies established by the MHCC-97H and LM3 cells, respectively (Supplementary Fig. 2D). Furthermore, knockdown of RRP15 markedly increased the apoptosis rates of both MHCC-97 H and LM3 cells (Supplementary Fig. 3A–B); and led to an elevated number of cells in the sub-G1 and G1 phases and a reduction in the number of cells in the G2/M phase (Supplementary Fig. 3C–D). Consistently, the lack of RRP15 upregulated P53 and attenuated PCNA, Cyclin D1 and CDK2 protein levels in both cell lines (Supplementary Fig. 3E). Collectively, the above results indicated that RRP15 knockdown suppressed the proliferation of HCC cells and attenuated tumorigenesis by inducing G1-phase arrest and apoptosis.

Additionally, in a nude mouse HCC xenograft model established using MHCC-97H cells, the tumor volume of RRP15 knockout nude mice was significantly reduced 15 days after inoculation compared to controls (Supplementary Fig. 3F). Consistent with this, RRP15 depletion also decreased the tumor weight (Supplementary Fig. 3G) and overall tumor size (Supplementary Fig. 3H) compared to that in the control group.

### RRP15 knockdown attenuated HCC migration and invasion independent of P53

The effect of RRP15 on HCC migration was also ascertained by shRNA-mediated knockdown in MHCC-97H and LM3 cells (Fig. 2A). And in the wound healing assay, inhibition of RRP15 remarkably reduced the migration of HCC cells (Fig. 2B). Furthermore, knocking down RRP15 markedly suppressed the migration and invasion of MHCC-97 H and LM3 cells in the transwell assay (Fig. 2C–D), and decreased the adhesion of HCC cells (Fig. 2E). EMT is a pivotal process of HCC migration [23], unsurprisingly, RRP15 knockdown promoted the expression of epithelial marker E-cadherin, and diminished the mesenchymal markers N-cadherin and matrix metalloproteinase (MMP) 9 in the HCC cell lines (Fig. 2F).

Since knockdown of RRP15 increased P53 expression, we hypothesized that RRP15 regulation of HCC migration dependent on P53. Thus, we used siRNA to block the expression of RRP15 in P53-deficient cell line

**Figure 1**

**Fig. 1** Upregulation of RRP15 in HCC tissues and cells. **(A)** The expression level of RRP15 mRNA in HCC tissues (T) and normal liver tissues (N) in the TCGA database. **(B)** Overall survival of HCC patients according to Kaplan-Meier database in the TCGA database. **(C, D)** The expression of RRP15 mRNA and protein in HCC tissues and adjacent non-tumor tissues. **(E)** Representative images and quantitative analysis of TMA stained with IHC for RRP15. Scale bar = 50  $\mu$ m. **(F, G)** RRP15 protein and mRNA levels in five HCC cell lines and a normal liver cell line. Data are presented as mean  $\pm$  SEM. \* $p < 0.05$ , \*\* $p < 0.01$ , \*\*\* $p < 0.001$ . RRP15: ribosomal RNA processing protein 15; HCC: hepatocellular carcinoma; TMA: tissue microarray

Hep3B (Supplementary Fig. 4A–B). The data revealed knockdown of RRP15 could also attenuate the migration, invasion, and adhesion of the Hep3B cells (Supplementary Fig. 4C–E), indicating that the regulation of RRP15 knockdown on the migration of HCC did not depend on the increase of P53 expression.

On the other hand, in a mouse lung migration model constructed by intravenously injecting MHCC-97 H cells, the number of lung metastatic nodules was obviously increased in mice injected with shNT cells compared

with those injected with shRRP15 cells (Fig. 2G, H), and aggressive tumor areas in the lung sections (Fig. 2I). In summary, knockdown of RRP15 attenuated HCC migration.

#### **Inhibition of RRP15 downregulated the focal adhesion pathway**

To further investigate the mechanisms underlying RRP15-mediated regulation of HCC migration, we analyzed the transcriptomic changes in MHCC-97H cells

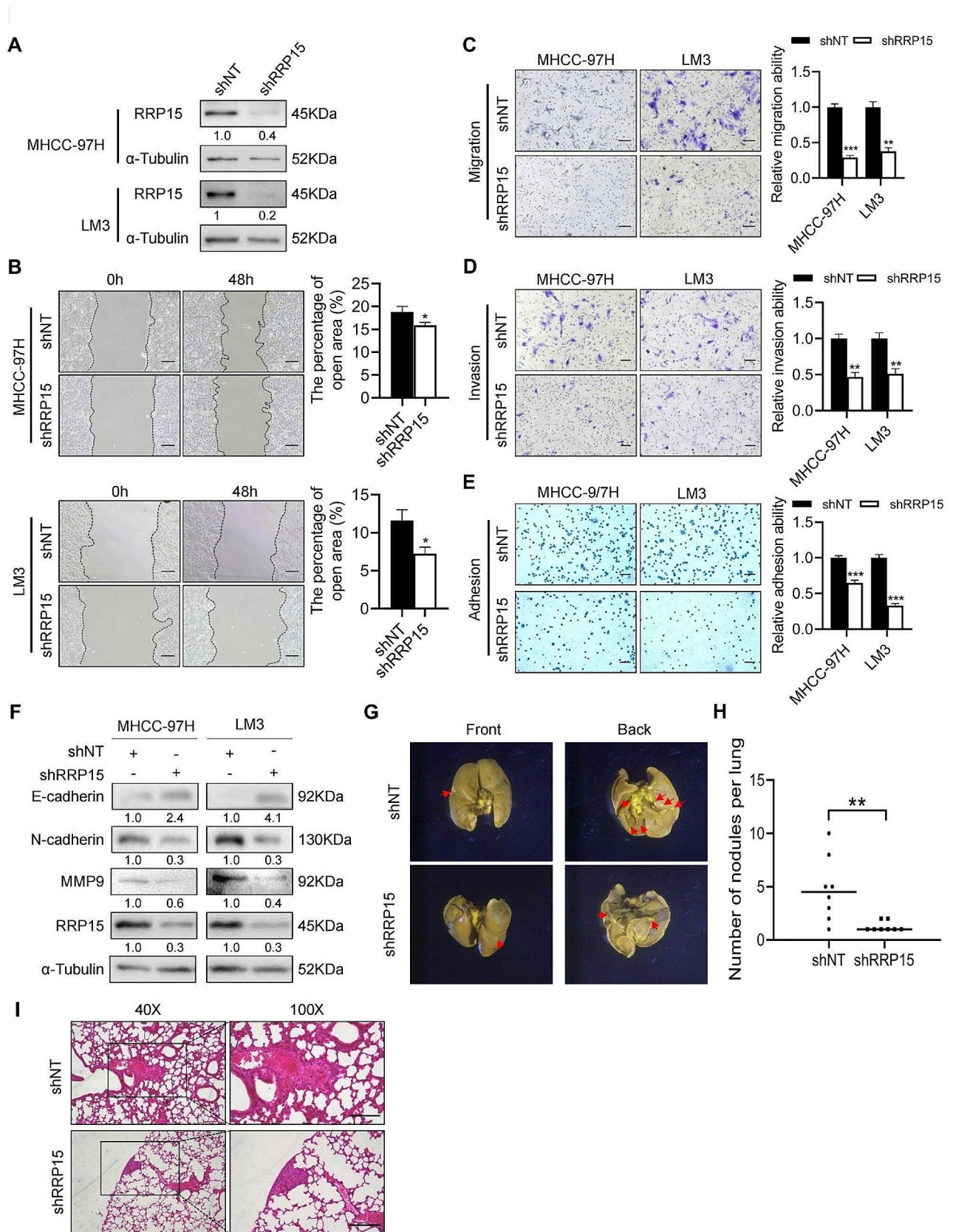


**Fig. 2** (See legend on next page.)

(See figure on previous page.)

**Fig. 2** RRP15 knockdown attenuated the migration and invasion of HCC. **(A)** The knockdown efficiency of RRP15 in HCC cells. **(B)** Downregulation of RRP15 inhibited migration of HCC cell in the wound healing assay. Scale bars = 100  $\mu$ m. **(C–D)** Migration and invasion of MHCC-97 H or LM3 cells transfected with shNT or shRRP15 in the transwell assay. Scale bars = 100  $\mu$ m. **(E)** Downregulation of RRP15 inhibited adhesion of HCC cells. Scale bars = 100  $\mu$ m. **(F)** Expression levels of EMT-related proteins in MHCC-97 H or LM3 cells transfected with shNT or shRRP15. **(G)** Representative images of lung metastases observed under a stereoscope. Scale bars = 1 cm. **(H)** Number of metastatic nodules in the lung tissues in the indicated groups ( $n=8$  per group). **(I)** Representative images of H&E-stained lung tissue sections in shNT/shRRP15 mice. Scale bars = 100  $\mu$ m. Data are presented as mean  $\pm$  SEM. \* $p < 0.05$ , \*\* $p < 0.01$ , \*\*\* $p < 0.001$ . RRP15: ribosomal RNA processing protein 15; HCC: hepatocellular carcinoma. H&E: hematoxylin and eosin

with a stable knockdown of RRP15. RNA sequencing revealed that compared to the control cells, the RRP15-knockdown cells had 350 up-regulated genes and 316 down-regulated genes were by two-fold (Fig. 3A). Moreover, Kyoto Encyclopedia of Genes and Genomes (KEGG) enrichment analysis showed that the differentially expressed genes were mainly associated with focal adhesion, complement and coagulation cascades, and ECM-receptor interaction (Fig. 3B). The focal adhesion pathway consists of multiple genes involved in cell motility and cancer metastasis [24], suggesting that RRP15 knockdown regulates the migration and invasion of HCC cells. Further screening for genes involved in focal adhesion and ECM-receptor interaction, we found that *COL1A1*, *COL4A5*, *COL4A6*, *HGF*, *TNC* and *PIP5K1C* genes were upregulated, whereas *PRKCG*, *TNXB*, *BIRC3*, *MAPK8*, *PDGFB*, *LAMC2*, *LAMB3*, *ITGA7*, *SHC2*, *ERBB2*, *ITGB3* and *LAMA3* were downregulated (Fig. 3C). *LAMA3*, *LAMC2* and *LAMB3* respectively encode for the  $\alpha 1$ ,  $\gamma 2$  and  $\beta 3$  chains of laminin-5 [25], which is a key factor involved in focal adhesion. RRP15 knockdown decreased *LAMC2*, *LAMB3* and *LAMA3* mRNA levels in the MHCC-97 H cells, and downregulated *LAMC2* and *LAMB3* in LM3 cells (Fig. 3D, E). In addition, RRP15 depletion also reduced *LAMC2* and *LAMB3* protein levels in both cell lines (Fig. 3F). Laminin-5 is the main ligand of integrin  $\alpha 6\beta 4$ , and the binding of integrin  $\beta 4$  to *LAMC2* facilitates tumor metastasis through FAK [26]. Consistent with this, knockdown of RRP15 decreased *ITGB4*, p-FAK, p-ERK and p-p65 NF- $\kappa$ B levels in the HCC cells (Fig. 3G).

#### RRP15 enhanced migration of HCC cells through the LAMC2/ITGB4/FAK pathway

To further determine whether RRP15 knockdown suppressed HCC migration in a *LAMC2*-dependent manner, we simultaneously overexpressed RRP15 and knocked down *LAMC2* in both cell lines (Fig. 4A, B), and found that overexpression of RRP15 increased *ITGB4* protein levels, and those of phosphorylated FAK, ERK and p65 NF- $\kappa$ B. Furthermore, knocking down *LAMC2* decreased FAK and p65 NF- $\kappa$ B phosphorylation and downregulated *ITGB4* in the RRP15-overexpressing HCC cells (Fig. 4C), but did not restore the levels of p-ERK. *LAMC2* knockdown also inhibited the migration of RRP15-overexpressing cells (Fig. 4D–E). Taken together, RRP15 knockdown

suppressed HCC migration by inhibiting the *ITGB4*/FAK/NF- $\kappa$ B signaling pathway through *LAMC2*.

#### RRP15 promoted the transcription of *LAMC2* and *LAMB3* through *PATZ1* in HCC cells

Given that RRP15 is mainly localized in the nucleus [15], it is possible that it acts as a transcription factor in the nucleus to regulate *LAMC2* and *LAMB3* gene expression. We identified the POZ/BTB and AT hook containing zinc finger 1 (*PATZ1*) in the common promoter region of *LAMC2* and *LAMB3* by JASPAR database analysis (Fig. 5A). *PATZ1* expression was positively correlated with that of RRP15, *LAMC2* and *LAMB3* in the TCGA database (Fig. 5B). Furthermore, despite comparable mRNA levels of *PATZ1*, stable knockdown of RRP15 in both cell lines decreased *PATZ1* expression (Fig. 5C). Therefore, we stably knocked down *PATZ1* in the MHCC-97 H and LM3 cells to explore its effect on RRP15-dependent regulation of HCC migration (Fig. 5D). While overexpressing RRP15 increased the expression of *LAMC2* and *LAMB3* mRNAs, knocking down *PATZ1* led to their downregulation in the RRP15-overexpressing HCC cells (Fig. 5E–F). Consistently, *PATZ1* knockdown prevented the migration of RRP15-overexpressing HCC cells (Fig. 5G). Overall, our data suggest that RRP15 promotes HCC migration via *PATZ1*-mediated transcriptional regulation of *LAMC2* and *LAMB3*.

#### Discussion

Zhao et al. showed that ablation of RRP15 prevented HCC proliferation and growth both in a p53-dependent manner in vitro and in vivo [19]. However, whether and how RRP15 affects the migration of HCC has not been studied so far. Since the high migration rates are responsible for the high mortality rate of patients with HCC [5–7], it is momentous to unearth new molecular markers that can accurately predict HCC migration. We innovatively found that high expression of RRP15 was associated with lower survival in HCC patients. Knocking down RRP15 expression prevented the proliferation, migration and invasion of HCC cells, independent of P53 expression, and also suppressed lung migration in a mouse model.

Laminin-5 is considerably associated with the growth, metastasis and prognosis of HCC tumors [27, 28]. It consists of the laminin  $\alpha 3$ ,  $\gamma 2$  and  $\beta 3$  subunits, which are encoded by *LAMA3*, *LAMC2* and *LAMB3* respectively

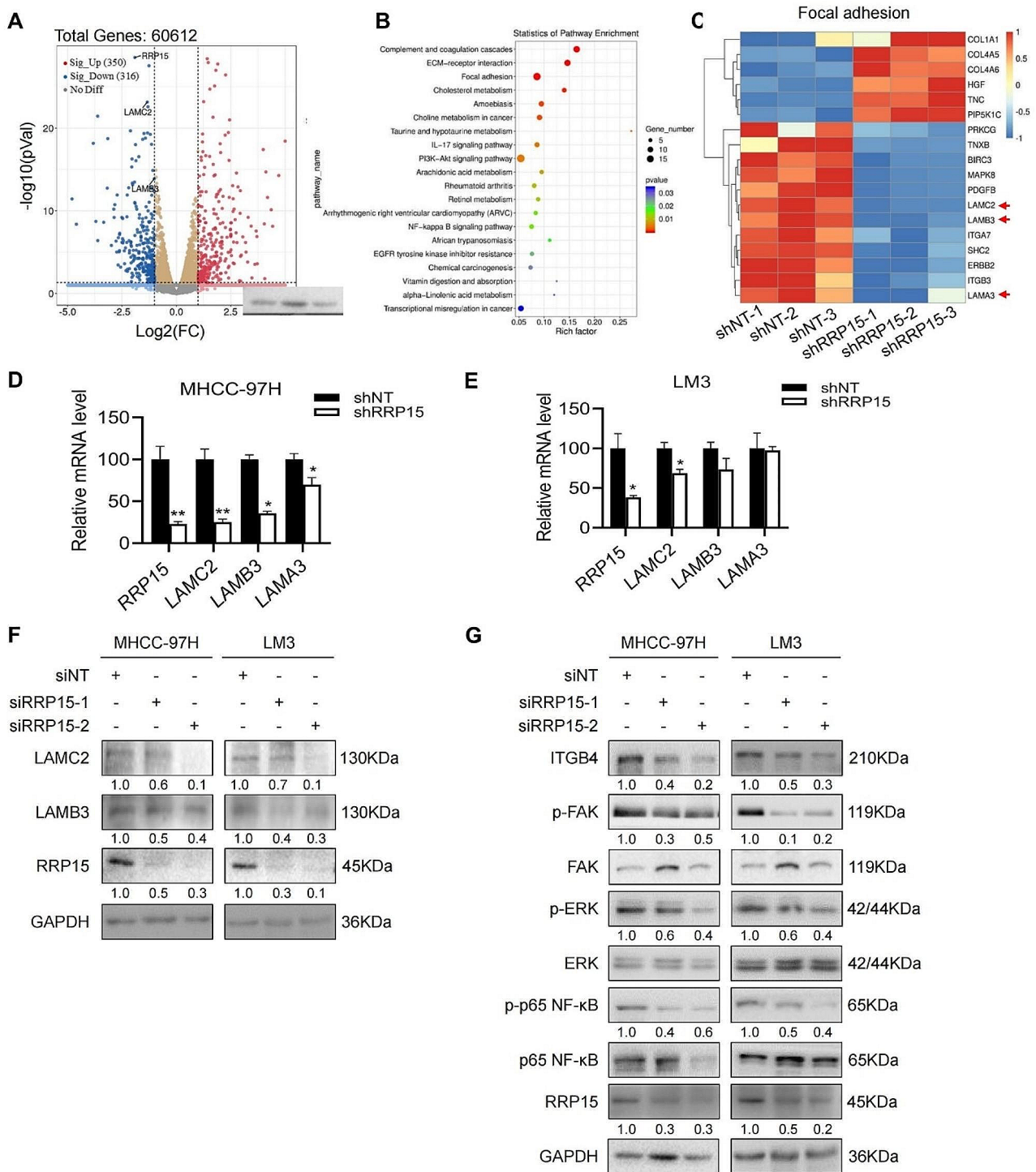


**Fig. 3** (See legend on next page.)

(See figure on previous page.)

**Fig. 3** RRP15 knockdown inactivated the LAMC2/ITGB4/FAK pathway in HCC cells. **(A)** The volcano plot of differentially expressed genes (DEGs). The blue dots represent downregulated genes, the grey dots are non-differentially expressed genes and the red dots are upregulated genes. **(B)** KEGG pathway analysis showing the significantly associated signaling pathways in the RRP15-knockdown MHCC-97 H cells. **(C)** Heatmap of DEGs. Up- and down-regulated genes are shown in red and blue respectively. **(D-E)** Effect of RRP15 knockdown on the expression of LAMC2, LAMB3 and LAMA3 mRNAs. **(F)** Effect of RRP15 knockdown on the expression of LAMC2 and LAMB3 proteins. **(G)** Immunoblots showing ITGB4, pFAK, pERK, p-p65, FAK, ERK and p65 levels in RRP15-knockdown and control cells. Data are presented as mean  $\pm$  SEM. \* $p < 0.05$ , \*\* $p < 0.01$ . RRP15: ribosomal RNA processing protein 15; LAMC2: laminin subunit gamma 2; ITGB4: integrin subunit beta 4; FAK: focal adhesion kinase; HCC: hepatocellular carcinoma; LAMB3: laminin subunit beta 3; ERK: mitogen-activated protein kinase 1

[25]. LAMC2 is overexpressed in multiple cancers and drives tumorigenesis by interacting with  $\alpha 6\beta 4$  and  $\alpha 3\beta 1$  integrins, epidermal growth factor receptor (EGFR), and other surface receptors [26, 27, 29–32]. In addition, deletion of LAMC2 suppressed the EMT and lymph node metastasis of cholangiocarcinoma via inactivation of the EGFR signaling pathway [33, 34]. LAMC2 is also overexpressed in ovarian cancer and can regulate tumor cell proliferation and metastasis [35]. We similarly found that RRP15 overexpression promoted the migration of HCC cells in vitro, and its oncogenic effect was abrogated by the simultaneous knockdown of LAMC2. Furthermore, the lack of RRP15 also decreased the expression of LAMC2 in HCC cells.

LAMC2 binds to integrins  $\alpha 6\beta 4$  and phosphorylates FAK, and activates downstream signaling pathways, such as those already reported in esophageal squamous cell carcinoma and breast cancer [26, 36–38]. FAK protein overexpression is highly associated with aggressive behavior and undesirable outcome in HCC [39, 40]. In colon cancer cells, FAK phosphorylation regulates E-cadherin expression by activating the Src signaling pathways [41]. Our results indicate that knockdown of RRP15 inhibited the FAK signaling pathway, whereas overexpression increased the level of phosphorylated FAK. LAMC2 knockdown attenuated FAK signaling in the RRP15-overexpressing cells. Furthermore, NF- $\kappa$ B, a downstream effector of FAK [42, 43], was also down-regulated by RRP15 knockdown. Altogether, these findings suggest that knockdown of RRP15 suppresses HCC migration via attenuation of LAMC2/FAK/NF- $\kappa$ B signaling.

In addition, we also found an interesting phenomenon that loss of RRP15 up-regulates the expression of fibrogenic genes, including *COL1A1*, *COL4A5* and *COL4A6*, suggesting that RRP15 may inhibit fibrosis. The role of tumor-associated fibrosis in cancer progression is inconclusive, and increasing evidence has revealed that tumor-associated fibrosis inhibits the development, proliferation and metastasis of cancer. Alkasalias et al. found that fibroblast fusion into monolayers effectively inhibited tumor cell proliferation in vitro [44]. Mechanistically, hedgehog, as a key signaling pathway that promotes fibrosis, may play an important role in stromal cells inhibiting tumor progression. For example, genetic and pharmacological inhibition of hedgehog accelerates the

progression of pancreatic and bladder cancers [45, 46]; hedgehog agonists induce stromal hyperplasia but reduce epithelial cell proliferation, thereby inhibiting cancer development [45]. However, the role of RRP15 in fibrosis has not been reported, and we speculate that RRP15 may also promote the progression of HCC by inhibiting fibrosis, but this speculation and the underlying mechanism need to be further studied.

Further, the predominantly nuclear location of RRP15 suggests that it may regulate gene expression [15]. Dong et al. showed that RRP15 promotes colorectal cancer metastasis through regulating leucine zipper tumor suppressor 2-mediated  $\beta$ -catenin signaling [17]. We found that RRP15 regulates downstream target genes at the transcriptional level, and RRP15 depletion attenuated LAMC2 expression, at least in part, through the inactivation of PAZT1 promoter. Nevertheless, we were unable to conclusively identify the mechanisms through which RRP15 regulates LAMC2, and the purported interaction between RRP15 and the transcription factor PATZ1 needs to be investigated further.

## Conclusions

RRP15, a potential HCC biomarker and therapeutic target, upregulates LAMC2 through the transcription factor PATZ1, which promotes the migration of HCC cells (Fig. 5H), whereas knockdown of RRP15 inhibits the migration of HCC by attenuating LAMC2/integrin  $\beta 4$ /FAK signaling.

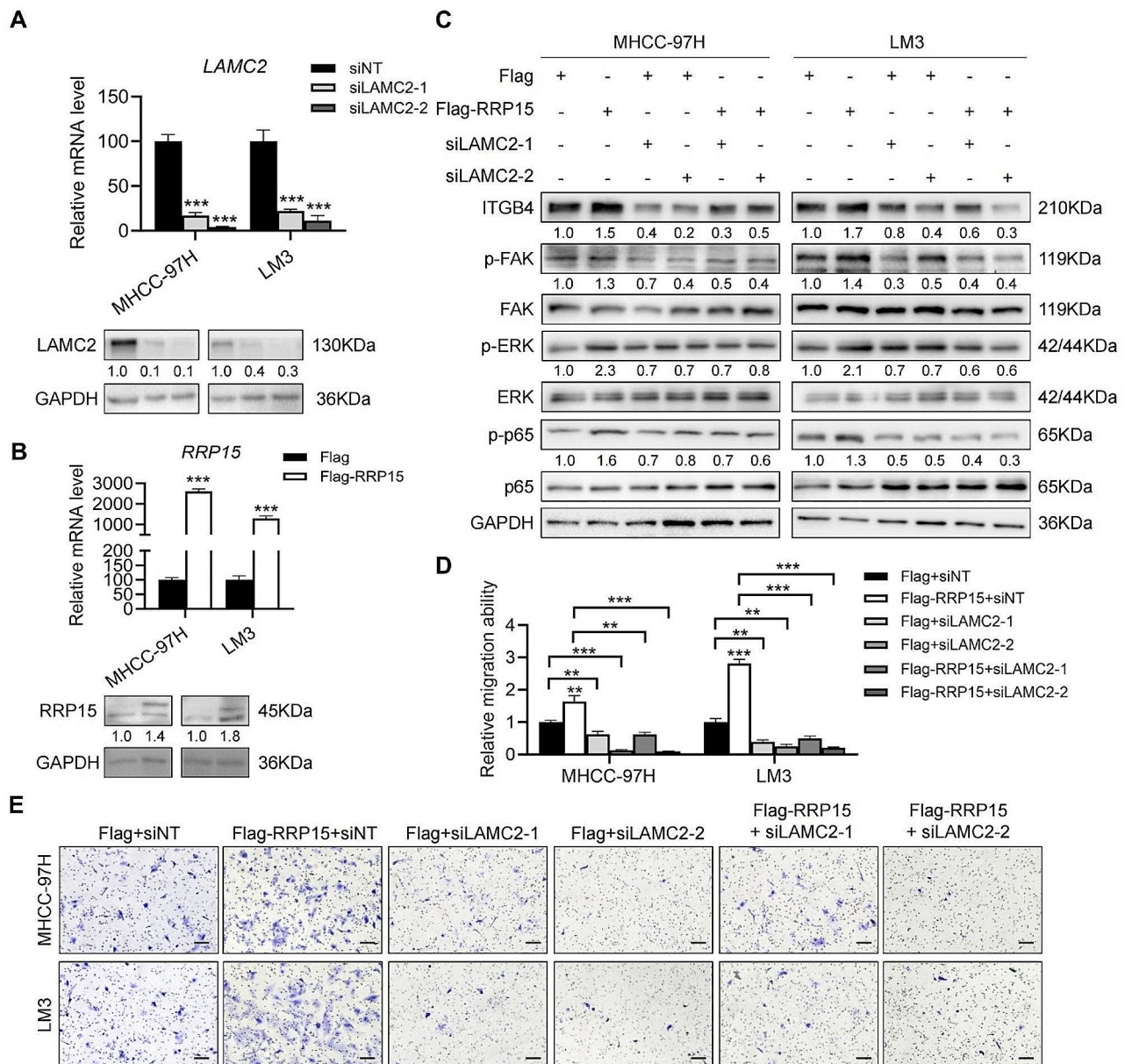


**Fig. 4** RRP15 enhanced migration of HCC cells through the LAMC2/ITGB4/FAK pathway. **(A)** The knockdown efficiency of LAMC2 in HCC cells. **(B)** The overexpression of RRP15 in HCC cells. **(C)** Expression levels of the indicated proteins in RRP15-overexpressing MHCC-97 H and LM3 cells with or without LAMC2 knockdown. **(D-E)** Migration and invasion of RRP15-overexpressing MHCC-97 H and LM3 cells with or without LAMC2 knockdown in the transwell assay. Scale bars= 100  $\mu$ m. Data are presented as mean  $\pm$  SEM. \* $p$ <0.05, \*\* $p$ <0.01, \*\*\* $p$ <0.001. RRP15: ribosomal RNA processing protein 15; LAMC2: laminin subunit gamma 2; ITGB4: integrin subunit beta 4; FAK: focal adhesion kinase; HCC: hepatocellular carcinoma

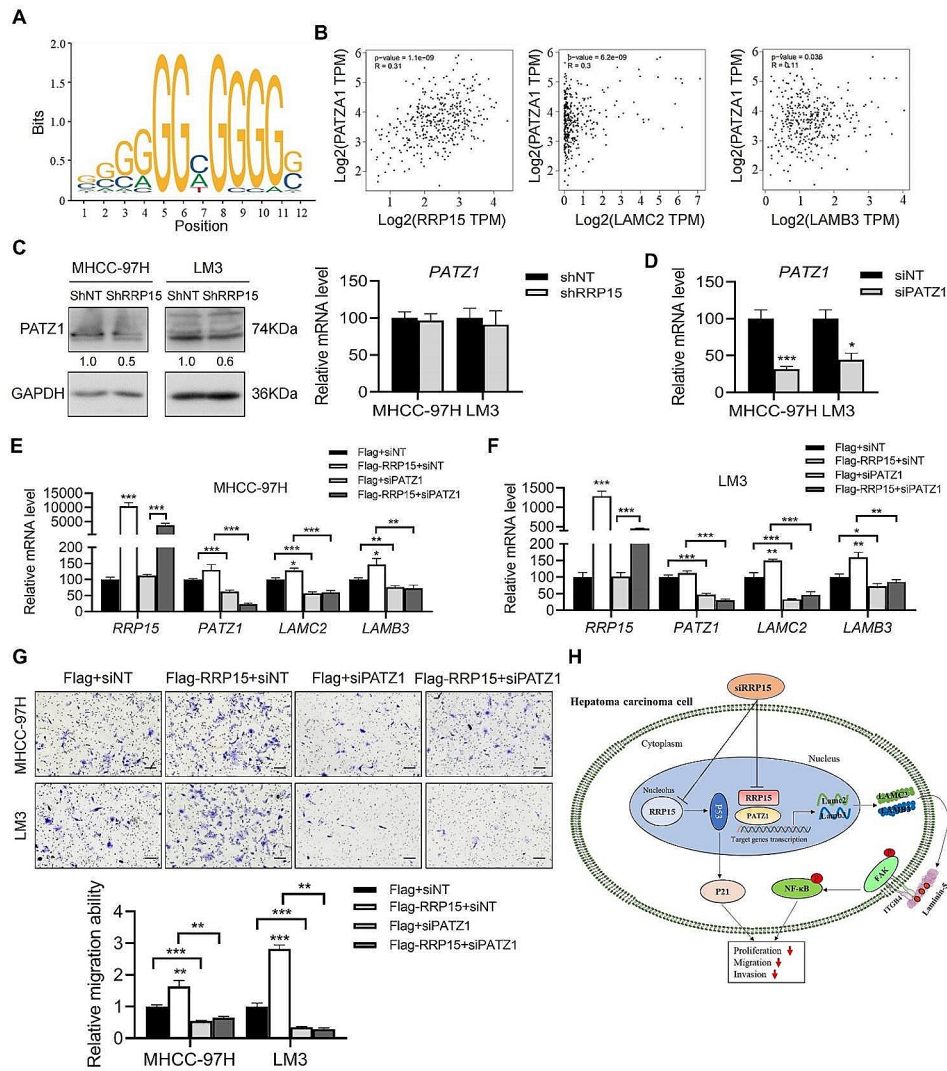


**Fig. 5** Knockdown PATZ1 suppressed LAMC2 and LAMB3 transcription in HCC cells. **(A)** Transcriptional binding site of PATZ1. **(B)** Correlation of PATZ1 mRNA level with RRP15, LAMC2 and LAMB3 mRNA levels. **(C)** Protein and mRNA levels of PATZ1 in RRP15 knockdown cells. **(D)** The knockdown efficiency of PATZ1 in HCC cells. **(E-F)** Expression levels of the indicated mRNAs in RRP15-overexpressing MHCC-97 H and LM3 cells with or without PATZ1 knockdown. **(G)** Migration and invasion of RRP15-overexpressing MHCC-97 H and LM3 cells with or without PATZ1 knockdown in the transwell assay. Scale bars = 100  $\mu$ m. **(H)** Schematic diagram showing that knockdown of RRP15 inhibits the growth and metastasis of HCC cells via inactivation of the LAMC2 / FAK signaling. Data are presented as means  $\pm$  SEM. \* $p < 0.05$ , \*\* $p < 0.01$ , \*\*\* $p < 0.001$ . PATZ1: POZ/BTB and AT hook containing zinc finger 1; LAMC2: laminin subunit gamma 2; LAMB3: laminin subunit beta 3; HCC: hepatocellular carcinoma

**Supplementary Information**

The online version contains supplementary material available at <https://doi.org/10.1186/s12885-024-12065-4>.

- Supplementary Material 1
- Supplementary Material 2

**Acknowledgements**

Not available.

**Author contributions**

T.P.: Investigation, Data curation, Clinical data collection. J.L., O.Z., Y.Z., H.Z., M.M. and Y.Y.: Investigation, Data curation, Visualization. J.L.: Clinical data collection. Y.C.: Clinical data collection, Resources. L.X.: Conceptualization, Methodology, Resources, Writing-Reviewing and Approval. All authors reviewed the manuscript.

## Funding

This study was supported by National Natural Science Foundation of China/81900778 (to LX); Natural Science Foundation of Zhejiang Province/LY21H070004, LD21H030002 (to LX and YC).

## Availability of data and material

The dataset supporting the conclusions of this article is available in the [GSE228416]. All data are available upon request from the corresponding author.

## Declarations

### Ethics approval and consent to participate

This study was conducted in accordance with the Declaration of Helsinki and approved by the Ethics Committee of Lishui People's Hospital (No. LLW-FO-401). All methods were carried out in accordance with relevant guidelines and regulations. All the informed consent was obtained from all subjects and/or their legal guardian(s).

The animal experiment program was authorized by the Wenzhou Medical University Animal Experiment Committee (No. wyd2022-0164). All experiments were conducted following the Guide for the Care and Use of Laboratory Animals (China), and reported according to ARRIVE guidelines (<https://arriveguidelines.org>).

### Consent for publication

Not applicable.

### Competing interests

The authors declare no competing interests.

### Author details

<sup>1</sup>Key Laboratory of Laboratory Medicine, Ministry of Education, School of Laboratory Medicine and Life Sciences, Wenzhou Medical University, 325035 Wenzhou, Zhejiang, China

<sup>2</sup>Zhejiang Provincial Key Laboratory for Accurate Diagnosis and Treatment of Chronic Liver Diseases, The First Affiliated Hospital of Wenzhou Medical University, 325035 Wenzhou, Zhejiang, China

<sup>3</sup>Department of Liver and Gall Surgery, The Third Affiliated Hospital of Wenzhou Medical University, 325200 Wenzhou, Zhejiang, China

<sup>4</sup>Department of Infectious Diseases, Lishui People's Hospital, 323000 Lishui, Zhejiang, China

Received: 4 November 2023 / Accepted: 27 February 2024

Published online: 12 March 2024

## References

- Sung H, Ferlay J, Siegel RL, Laversanne M, Soerjomataram I, Jemal A, Bray F. Global cancer statistics 2020: GLOBOCAN estimates of incidence and mortality worldwide for 36 cancers in 185 countries. *CA Cancer J Clin*. 2021;71(3):209–49.
- Malek NP, Schmidt S, Huber P, Manns MP, Greten TF. The diagnosis and treatment of hepatocellular carcinoma. *Dtsch Arztebl Int*. 2014;111(7):101–6.
- Forner A, Reig M, Bruix J. Hepatocellular carcinoma. *Lancet (London England)*. 2018;391(10127):1301–14.
- Dhir M, Melin AA, Douaiher J, Lin C, Zhen WK, Hussain SM, Geschwind JF, Doyle MB, Abou-Alfa GK, Are C. A review and update of treatment options and controversies in the management of hepatocellular carcinoma. *Ann Surg*. 2016;263(6):1112–25.
- Natsuzaka M, Omura T, Akaike T, Kuwata Y, Yamazaki K, Sato T, Karino Y, Toyota J, Suga T, Asaka M. Clinical features of hepatocellular carcinoma with extrahepatic metastases. *J Gastroenterol Hepatol*. 2005;20(11):1781–7.
- Obenauf AC, Massagué J. Surviving at a Distance: Organ-Specific Metastasis. *Trends Cancer*. 2015;1(1):76–91.
- Katyal S, Oliver JH, Peterson MS, Ferris JV, Carr BS, Baron RL. Extrahepatic metastases of hepatocellular carcinoma. *Radiology*. 2000;216(3):698–703.
- Gkretsi V, Stylianopoulos T. Cell adhesion and matrix stiffness: coordinating cancer cell invasion and metastasis. *Front Oncol*. 2018;8:145.
- Walker C, Mojares E, Del Río Hernández A. Role of extracellular matrix in development and cancer progression. *Int J Mol Sci* 2018, 19(10).
- Holle AW, Young JL, Spatz JP. In vitro cancer cell-ECM interactions inform in vivo cancer treatment. *Adv Drug Deliv Rev*. 2016;97:270–9.
- Colognato H, Yurchenco PD. Form and function: the laminin family of heterotrimers. *Dev Dyn*. 2000;218(2):213–34.
- Kim SH, Turnbull J, Guimond S. Extracellular matrix and cell signalling: the dynamic cooperation of integrin, proteoglycan and growth factor receptor. *J Endocrinol*. 2011;209(2):139–51.
- Lu XS, Sun W, Ge CY, Zhang WZ, Fan YZ. Contribution of the PI3K/MMPs/Ln-5y2 and EphA2/FAK/Paxillin signaling pathways to tumor growth and vasculogenic mimicry of gallbladder carcinomas. *Int J Oncol*. 2013;42(6):2103–15.
- Nikolopoulos SN, Blaikie P, Yoshioka T, Guo W, Puri C, Tacchetti C, Giancotti FG. Targeted deletion of the integrin beta4 signaling domain suppresses laminin-5-dependent nuclear entry of mitogen-activated protein kinases and NF-kappaB, causing defects in epidermal growth and migration. *Mol Cell Biol*. 2005;25(14):6090–102.
- Dong Z, Zhu C, Zhan Q, Jiang W. The roles of RRP15 in nucleolar formation, ribosome biogenesis and checkpoint control in human cells. *Oncotarget*. 2017;8(8):13240–52.
- Ferguson B, Handoko HY, Mukhopadhyay P, Chitsazan A, Balmer L, Morahan G, Walker GJ. Different genetic mechanisms mediate spontaneous versus UVR-induced malignant melanoma. *Elife* 2019, 8.
- Dong Z, Lij, Dai W, Yu D, Zhao Y, Liu S, Li X, Zhang Z, Zhang R, Liang X, Kong Q, Jin S, Jiang H, Jiang W, Ding C. RRP15 deficiency induces ribosome stress to inhibit colorectal cancer proliferation and metastasis via LZTS2-mediated  $\beta$ -catenin suppression. *Cell Death Dis*, 89 (2023).
- Deng Z, Xu Y, Cai Y, Lin W, Zhang L, Jiang A, Zhou Y, Zhao R, Zhao H, Liu Z, Yan T. Inhibition of ribosomal RNA processing 15 homolog (RRP15) suppressed tumor growth, invasion and epithelial to mesenchymal transition (EMT) of colon cancer. *Int J Mol Sci*, 24(4):3528.
- Zhao D, Qian L, Zhuang D, Wang L, Cao Y, Zhou F, Zhang S, Liu Y, Liang Y, Zhang W, et al. Inhibition of ribosomal RNA processing 15 homolog (RRP15), which is overexpressed in hepatocellular carcinoma, suppresses tumour growth via induction of senescence and apoptosis. *Cancer Lett*. 2021;519:315–27.
- Wei C, Wang B, Chen ZH, Xiao H, Tang L, Guan JF, Yuan RF, Yu X, Hu ZG, Wu HJ, et al. Validating RRP12 expression and its prognostic significance in HCC based on data mining and bioinformatics methods. *Front Oncol*. 2022;12:812009.
- Zhou Y, Xu Q, Tao L, Chen Y, Shu Y, Wu Z, Lu C, Shi Y, Bu H. Enhanced SMARCD1, a subunit of the SWI/SNF complex, promotes liver cancer growth through the mTOR pathway. *Clin Sci (Lond)*. 2020;134(12):1457–72.
- Dong Y, Zheng Q, Wang Z, Lin X, You Y, Wu S, Wang Y, Hu C, Xie X, Chen J, et al. Higher matrix stiffness as an independent initiator triggers epithelial-mesenchymal transition and facilitates HCC metastasis. *J Hematol Oncol*. 2019;12(1):112.
- Diepenbruck M, Christofori G. Epithelial-mesenchymal transition (EMT) and metastasis: yes, no, maybe? *Curr Opin Cell Biol*. 2016;43:7–13.
- Sulzmaier FJ, Jean C, Schlaepfer DD. FAK in cancer: mechanistic findings and clinical applications. *Nat Rev Cancer*. 2014;14(9):598–610.
- Miyazaki K. Laminin-5 (laminin-332): unique biological activity and role in tumor growth and invasion. *Cancer sci*. 2006;97(2):91–8.
- Liang Y, Chen X, Wu Y, Li J, Zhang S, Wang K, Guan X, Yang K, Bai Y. LncRNA CAS9 promotes esophageal squamous cell carcinoma metastasis through upregulating LAMC2 expression by interacting with the CREB-binding protein. *Cell Death Differ*. 2018;25(11):1980–95.
- Bergamini C, Sgarra C, Trerotoli P, Lupo L, Azzariti A, Antonaci S, Giannelli G. Laminin-5 stimulates hepatocellular carcinoma growth through a different function of alpha6beta4 and alpha3beta1 integrins. *Hepatology*. 2007;46(6):1801–9.
- Giannelli G, Bergamini C, Fransvea E, Marinosci F, Quaranta V, Antonaci S. Human hepatocellular carcinoma (HCC) cells require both alpha3beta1 integrin and matrix metalloproteinases activity for migration and invasion. *Lab Invest*. 2001;81(4):613–27.
- Takahashi S, Hasebe T, Oda T, Sasaki S, Kinoshita T, Konishi M, Ochiai T, Ochiai A. Cytoplasmic expression of laminin gamma2 chain correlates with post-operative hepatic metastasis and poor prognosis in patients with pancreatic ductal adenocarcinoma. *Cancer*. 2002;94(6):1894–901.
- Smith SC, Nicholson B, Nitz M, Frierson HF Jr, Smolkin M, Hampton G, El-Rifai W, Theodorescu D. Profiling bladder cancer organ site-specific metastasis identifies LAMC2 as a novel biomarker of hematogenous dissemination. *Am J Pathol*. 2009;174(2):371–9.

31. Garg M, Kanojia D, Okamoto R, Jain S, Madan V, Chien W, Sampath A, Ding LW, Xuan M, Said JW, et al. Laminin-5 $\gamma$ -2 (LAMC2) is highly expressed in anaplastic thyroid carcinoma and is associated with tumor progression, migration, and invasion by modulating signaling of EGFR. *J Clin Endocrinol Metab.* 2014;99(1):E62–72.
32. Kosanam H, Prassas I, Chrystoja CC, Soleas I, Chan A, Dimitromanolakis A, Blasutig IM, Rückert F, Gruetzmann R, Pilarsky C, et al. Laminin, gamma 2 (LAMC2): a promising new putative pancreatic cancer biomarker identified by proteomic analysis of pancreatic adenocarcinoma tissues. *Mol Cell Proteom.* 2013;12(10):2820–32.
33. Pei YF, Liu J, Cheng J, Wu WD, Liu XQ. Silencing of LAMC2 reverses epithelial-mesenchymal transition and inhibits angiogenesis in cholangiocarcinoma via inactivation of the epidermal growth factor receptor signaling pathway. *Am J Pathol.* 2019;189(8):1637–53.
34. Zhang D, Guo H, Feng W, Qiu H. LAMC2 regulated by microRNA-125a-5p accelerates the progression of ovarian cancer via activating p38 MAPK signaling. *Life Sci.* 2019;232:116648.
35. Daisuke H, Kato H, Fukumura K, Mayeda A, Miyagi Y, Seiki M, Koshikawa N. Novel LAMC2 fusion protein has tumor-promoting properties in ovarian carcinoma. *Cancer Sci.* 2021;112(12):4957–67.
36. Kim BG, Gao MQ, Choi YP, Kang S, Park HR, Kang KS, Cho NH. Invasive breast cancer induces laminin-332 upregulation and integrin  $\beta$ 4 neoexpression in myofibroblasts to confer an anoikis-resistant phenotype during tissue remodeling. *Breast Cancer Res.* 2012;14(3):R88.
37. Leng C, Zhang ZG, Chen WX, Luo HP, Song J, Dong W, Zhu XR, Chen XP, Liang HF, Zhang BX. An integrin beta4-EGFR unit promotes hepatocellular carcinoma lung metastases by enhancing anchorage independence through activation of FAK-AKT pathway. *Cancer Lett.* 2016;376(1):188–96.
38. Xu L, Hou Y, Tu G, Chen Y, Du YE, Zhang H, Wen S, Tang X, Yin J, Lang L, et al. Nuclear Drosha enhances cell invasion via an EGFR-ERK1/2-MMP7 signaling pathway induced by dysregulated miRNA-622/197 and their targets LAMC2 and CD82 in gastric cancer. *Cell Death Dis.* 2017;8(3):e2642.
39. Panera N, Crudele A, Romito I, Gnani D, Alisi A. Focal adhesion kinase: insight into molecular roles and functions in hepatocellular carcinoma. *Int J Mol Sci.* 2017, 18(1).
40. Yuan Z, Zheng Q, Fan J, Ai KX, Chen J, Huang XY. Expression and prognostic significance of focal adhesion kinase in hepatocellular carcinoma. *J Cancer Res Clin Oncol.* 2010;136(10):1489–96.
41. Yoon H, Dehart JP, Murphy JM, Lim ST. Understanding the roles of FAK in cancer: inhibitors, genetic models, and new insights. *J Histochem Cytochem.* 2015;63(2):114–28.
42. Dia VP, Gonzalez de Mejia E. Lunasin potentiates the effect of oxaliplatin preventing outgrowth of colon cancer metastasis, binds to  $\alpha$ 5 $\beta$ 1 integrin and suppresses FAK/ERK/NF- $\kappa$ B signaling. *Cancer Lett.* 2011;313(2):167–80.
43. Tan TW, Lai CH, Huang CY, Yang WH, Chen HT, Hsu HC, Fong YC, Tang CH. CTGF enhances migration and MMP-13 up-regulation via  $\alpha$ 5 $\beta$ 3 integrin, FAK, ERK, and NF- $\kappa$ B-dependent pathway in human chondrosarcoma cells. *J Cell Biochem.* 2009;107(2):345–56.
44. Flaberg E, Guven H, Savchenko A, Pavlova T, Kashuba V, Szekely L, Klein G. The architecture of fibroblast monolayers of different origin differentially influences tumor cell growth. *Int J Cancer.* 2012;131(10):2274–83.
45. Lee JJ, Perera RM, Wang H, Wu D-C, Liu XS, Han S, Fitamant J, Jones PD, Ghanta KS, Kawano S, et al. Stromal response to hedgehog signaling restrains pancreatic cancer progression. *Proc Natl Acad Sci U S A.* 2014;111(30):E3091–100.
46. Shin K, Lim A, Zhao C, Sahoo D, Pan Y, Spiekeroetter E, Liao JC, Beachy PA. Hedgehog signaling restrains bladder cancer progression by eliciting stromal production of urothelial differentiation factors. *Cancer Cell.* 2014;26(4):521–33.

#### Publisher's Note

Springer Nature remains neutral with regard to jurisdictional claims in published maps and institutional affiliations.